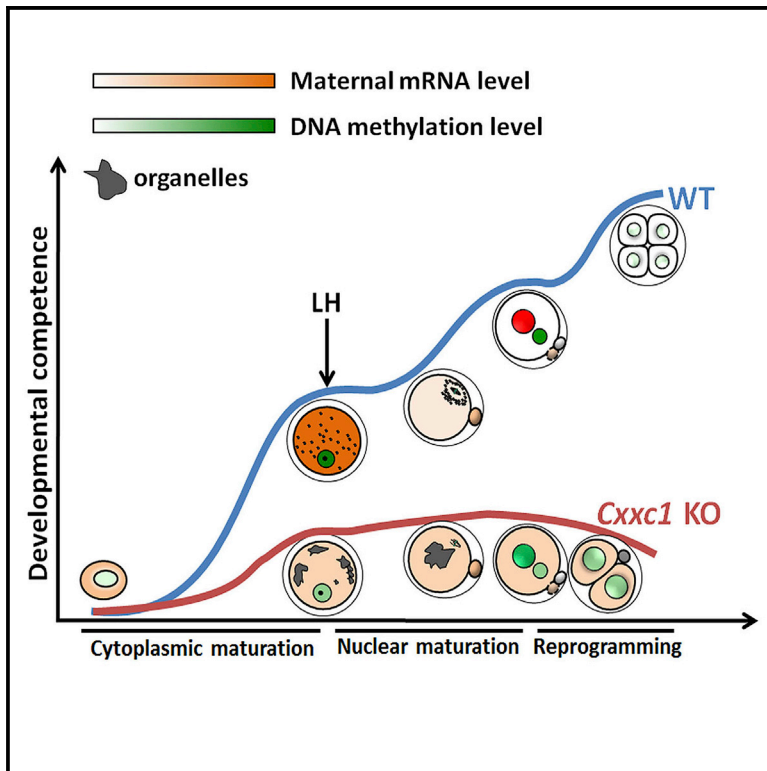


## CFP1 Regulates Histone H3K4 Trimethylation and Developmental Potential in Mouse Oocytes

### Graphical Abstract



### Authors

Chao Yu, Xiaoying Fan, Qian-Qian Sha, ..., Kui Liu, Fuchou Tang, Heng-Yu Fan

### Correspondence

hyfan@zju.edu.cn

### In Brief

Yu et al. define CFP1 as a key regulator of oocyte chromatin changes and developmental potential. Deletion of CFP1 in oocytes causes decreased H3K4me3 levels and transcription, in turn, leading to cytoskeletal defects, meiotic division, maternal-zygotic transition, and, ultimately, infertility.

### Highlights

- CFP1 regulates H3K4 trimethylation in developing oocytes
- Histone modification changes in oocytes rely on maternal CFP1
- CFP1-mediated H3K4me3 is crucial for oocyte transcription
- Deletion of CFP1 leads to decreased developmental competence and defects in MZT

### Accession Numbers

GSE85019



# CFP1 Regulates Histone H3K4 Trimethylation and Developmental Potential in Mouse Oocytes

Chao Yu,<sup>1,3,6</sup> Xiaoying Fan,<sup>2,6</sup> Qian-Qian Sha,<sup>1,6</sup> Hui-Han Wang,<sup>1</sup> Bo-Tai Li,<sup>1</sup> Xing-Xing Dai,<sup>1</sup> Li Shen,<sup>1</sup> Junping Liu,<sup>4</sup> Lie Wang,<sup>5</sup> Kui Liu,<sup>3</sup> Fuchou Tang,<sup>2</sup> and Heng-Yu Fan<sup>1,4,7,\*</sup>

<sup>1</sup>Life Sciences Institute, Zhejiang University, Hangzhou 310058, China

<sup>2</sup>Biomedical Institute for Pioneering Investigation via Convergence, Peking University, Beijing 100871, China

<sup>3</sup>Department of Chemistry and Molecular Biology, Goteborg University, Goteborg SE405 30, Sweden

<sup>4</sup>Institute of Aging Research, Hangzhou Normal University, Hangzhou 311121, China

<sup>5</sup>Institute of Immunology, Zhejiang University Medical School, Hangzhou 310058, China

<sup>6</sup>These authors contributed equally

<sup>7</sup>Lead Contact

\*Correspondence: [hyfan@zju.edu.cn](mailto:hyfan@zju.edu.cn)

<http://dx.doi.org/10.1016/j.celrep.2017.07.011>

## SUMMARY

Trimethylation of histone H3 at lysine-4 (H3K4me3) is associated with eukaryotic gene promoters and poises their transcriptional activation during development. To examine the *in vivo* function of H3K4me3 in the absence of DNA replication, we deleted CXXC finger protein 1 (CFP1), the DNA-binding subunit of the SETD1 histone H3K4 methyltransferase, in developing oocytes. We find that CFP1 is required for H3K4me3 accumulation and the deposition of histone variants onto chromatin during oocyte maturation. Decreased H3K4me3 in oocytes caused global downregulation of transcription activity. Oocytes lacking CFP1 failed to complete maturation and were unable to gain developmental competence after fertilization, due to defects in cytoplasmic lattice formation, meiotic division, and maternal-zygotic transition. Our study highlights the importance of H3K4me3 in continuous histone replacement for transcriptional regulation, chromatin remodeling, and normal developmental progression in a non-replicative system.

## INTRODUCTION

Mammalian oocytes undergo drastic epigenetic changes during development. This coincides with their role in preserving genetic and epigenetic information over an extended time span and transferring these attributes to the next generation (LaVoie, 2005; Lucifero et al., 2002; Schaefer et al., 2007). Histone modifications and histone exchange ensure the appropriate expression of genes involved in oogenesis in the absence of DNA replication and poise the zygotic genome for transcriptional activation after fertilization. However, little is known about the key factors regulating these DNA replication-independent changes and establishing oocyte developmental competence.

Histone H3 trimethylated at lysine-4 (H3K4me3) is linked to active versus inactive regions of the genome and is crucial for

embryonic stem cell (ESC) differentiation (Barrera et al., 2008; Zhao et al., 2007). During oogenesis and preimplantation embryogenesis, H3K4me3 is precisely regulated and its dynamics control the onset of these processes and developmental competence (Aoshima et al., 2015; Dahl et al., 2016; Liu et al., 2016a; Zhang et al., 2016). The SETD1 histone methyltransferase complex is reported to catalyze H3K4 trimethylation in many somatic cell types, but its function in germ cells is unclear (Tate et al., 2010). CXXC finger protein-1 (CFP1), encoded by the *Cxxc1* gene in mice, is a key component of the eukaryotic SETD1 complex (Clouaire et al., 2012; Lee and Skalnik, 2005). CFP1 binds to DNA using its CXXC finger domain and recruits SETD1 to specific genome regions (Thomson et al., 2010). Loss of the *Cxxc1* gene in mice results in early embryonic lethality, thus preventing the investigation of CFP1 function in later developmental processes, including oogenesis (Carlone and Skalnik, 2001).

Histone modifications are associated with the exchanges of histone variants, which are involved in the processes of DNA damage repair, transcription, and heterochromatin formation (Lin et al., 2014). The deposition of histones H3.1 and H3.2 onto chromatin depends on DNA replication. In contrast, H3.3, H4, and H2AX are deposited onto chromatin through DNA replication-uncoupled pathways (Akiyama et al., 2011; Nashun et al., 2015). H3.1 is enriched in dimethylated H3 lysine-9 (H3K9me2), whereas H3.3 is enriched in H3K4me3 (Akiyama et al., 2011). However, the role of CFP1-mediated H3K4 trimethylation in deposition dynamics of histone variants remains unclear *in vivo*.

To address these questions, we took advantage of oocyte-specific *Cxxc1* knockout mice. Postnatal mammalian oocytes are under cell-cycle arrest but nevertheless execute the oogenesis-specific developmental program, involving widespread transcriptional changes, active histone replacement, and *de novo* DNA methylation, ultimately acquiring competence, following fertilization, for zygotic genome activation (ZGA) (Ancelin et al., 2016).

We present evidence that CFP1 controls global H3K4me3 levels in mouse oocytes and is essential for female fertility. Conditional deletion of *Cxxc1* in growing oocytes substantially compromises histone exchange, DNA methylation, and transcriptional activity of the oocyte genome. Furthermore, decreases in maternal



H3K4me3 impair maternal-zygotic transition (MZT) and *de novo* histone deposition and prevent zygotic genome activation after fertilization.

## RESULTS

### Maternal CFP1 Deletion Leads to Decreased H3K4me3 in Oocytes and Zygotes

H3K4me3 level was low in growing mouse non-surrounded nucleus (NSN) oocytes, but was significantly increased in fully grown surrounded nucleus (SN) oocytes (Figure S1A), suggesting that H3K4me3 accumulation is an important aspect of oocyte epigenetic maturation. After ovulation, H3K4me3 localized to the condensed chromosomes in metaphase II (MII)-arrested oocytes and was inherited by the female pronucleus after fertilization (Figure S1A). Strikingly, H3K4me3 levels decreased during development from the 2-cell to 4-cell stages but increased again after the 4-cell stage (Figure S1A). The levels of mono- and di-H3K4 methylation (H3K4me1 and H3K4me2) showed a similar pattern with H3K4me3 in oocytes and preimplantation embryos (Figures S1B and S1C). Consistently, CFP1 was expressed and localized to the germinal vesicle (GV) of oocytes, from the primordial follicle to preovulatory follicle stages (Figure S2A). The CFP1 expression level was decreased, and its nuclear localization became non-significant after fertilization (Figures S2B and S2D). Consistent with the increase of H3K4me3 in early embryos, it was not until the 8-cell stage that CFP1 re-entered the nuclei (Figure S2B).

We crossed *Cxhc1*-floxed mice (*Cxhc1<sup>fl/fl</sup>*) with *Zp3-Cre* transgenic mice to delete *Cxhc1* in growing oocytes (Figure 1A). Immunohistochemistry (IHC) analysis in the ovaries of the *Cxhc1<sup>fl/fl</sup>;Zp3-Cre* females indicated that CFP1 was absent only in the oocytes of activated follicles (Figure 1B). No pups were born by *Cxhc1<sup>fl/fl</sup>;Zp3-Cre* females ( $n > 6$ , started at 2 months after birth) when crossed to wild-type (WT) males for at least 6 months.

H3K4me3 level was low in oocytes of primordial, primary, and secondary follicles but significantly increased in oocytes of antral follicles before ovulation (Figures 1C and S1A). The H3K4me3 level was decreased in the activated oocytes of *Cxhc1<sup>fl/fl</sup>;Zp3-Cre* mice (Figure 1C). Decrease of H3K4me3 level was also found in isolated CFP1-deleted oocytes (GV and MII) and zygotes, relative to the WT controls (Figures 1D and 1E). In a rescue experiment, CFP1-GFP expression partially restored H3K4me3 in CFP1-deleted NSN oocytes isolated from *Cxhc1<sup>fl/fl</sup>;Zp3-Cre* mice at postnatal day (PD) 12 but had few effects on fully grown SN oocytes isolated from *Cxhc1<sup>fl/fl</sup>;Zp3-Cre* mice at PD21 (Figures S3A–S3C). Moreover, the SN rate of oocytes derived from *Cxhc1<sup>fl/fl</sup>;Zp3-Cre* females (48%,  $n = 23$ ) was much lower than oocytes derived from WT oocytes (67%,  $n = 39$ ), at PD21–23. This result indicates that CFP1 mainly promotes H3K4me3 in growing oocytes during their epigenetic maturation.

Immunofluorescence (IF) staining and western blotting showed that the mono- and di-methylation of H3K4 in oocytes (PD21) were not affected by CFP1 deletion (Figures S3D, S3E, and S3G). In addition, trimethylation of H3K9 (H3K9me3) level was similar in WT and CFP1-deleted oocytes (Figure S3F). These results further suggest that CFP1 specifically regulates H3K4 trimethylation in oocytes.

### CFP1 and H3K4me3 Promote Oocyte Chromatin Accessibility and Transcriptional Activity

Results of the 5'-ethynyl uridine (EU) incorporation assay indicated that the overall genome transcriptional activity was greatly decreased in growing CFP1-deleted oocytes (Figure 2A). Dynamic histone exchanges are essential for maintaining normal transcriptional activity of the oocyte genome. Therefore, we performed histone replacement experiments by injecting mRNAs encoding FLAG-tagged histone variants into WT and CFP1-deleted oocytes. After an overnight culture, histones H3.3 and H2AX, but not H3.1, were remarkably incorporated into the oocyte chromatin (Figures 2B and 2C). However, the histone incorporation activities were significantly decreased in the CFP1-deleted oocytes (Figures 2B–2D). The newly translated FLAG-histone H3.3 underwent remarkable *de novo* trimethylation at lysine-4 in WT oocytes, but not in CFP1-deleted oocytes (Figure 2E). To assess the effect of CFP1 on oocyte chromatin accessibility, we incubated the WT and CFP1-deleted oocytes with DNase I of varied concentrations and measured the DNA double-strand breaks using a terminal deoxynucleotidyl transferase (TdT)-mediated dUTP nick end labeling (TUNEL) assay. The genomic DNA of CFP1-deleted oocytes was more resistant to DNase I digestion at each given DNase I concentration (Figures 2F and 2G). These results indicate that CFP1-mediated H3K4 trimethylation is essential for maintaining proper chromatin accessibility to protein factors that facilitate transcription during oocyte development.

### CFP1 Deletion Impairs the Expression of a Wide Range of Maternal Genes

We next profiled the whole-genome transcription of oocytes derived from WT and *Cxhc1<sup>fl/fl</sup>;Zp3-Cre* females. Samples of GV oocytes and zygotes of both genotypes (WT and *Cxhc1<sup>fl/fl</sup>;Zp3-Cre*) were subjected to RNA sequencing (RNA-seq) analyses, and the gene expression levels were assessed by fragments per kilobase of transcript per million mapped reads (FPKM), and the absolute mRNA copy number was evaluated with incorporated External RNA Controls Consortium (ERCC). We detected 13,113–15,872 transcripts (FPKM >0.1) from all samples, and all replicates showed high correlations ( $R \geq 0.98$ ; Figures 3A and S4A; Table S1). As shown in Figure 3B, there was a sharp decrease in the total mRNA copy number in CFP1-deleted oocytes, suggesting that CFP1 are crucial for maternal mRNA synthesis. Although there was a 40% decrease of whole-transcriptome amount in the CFP1-deleted GV oocytes, we observed more genes with increased mRNA copy number (718, fold change >2,  $p$  value <0.05, false discovery rate [FDR] <0.05) than those with decreased mRNA copy number (382, fold change <0.5,  $p$  value <0.05, FDR <0.05) in CFP1-deleted oocytes when compared with WT oocytes. Although the CFP1-deleted oocytes had more genes with increased mRNA copy number, these genes showed less abundance and moderate increase while the decreased genes were more abundant and downregulated significantly (Figure 3C). We also divided transcripts with FPKM >0.1 into ten bins according to their expression levels in WT oocytes and found that CFP1 globally affected gene transcription, regardless of transcript abundance (Figure 3D). The decreased expression of selected genes in the CFP1-deleted oocytes was extracted from RNA-seq

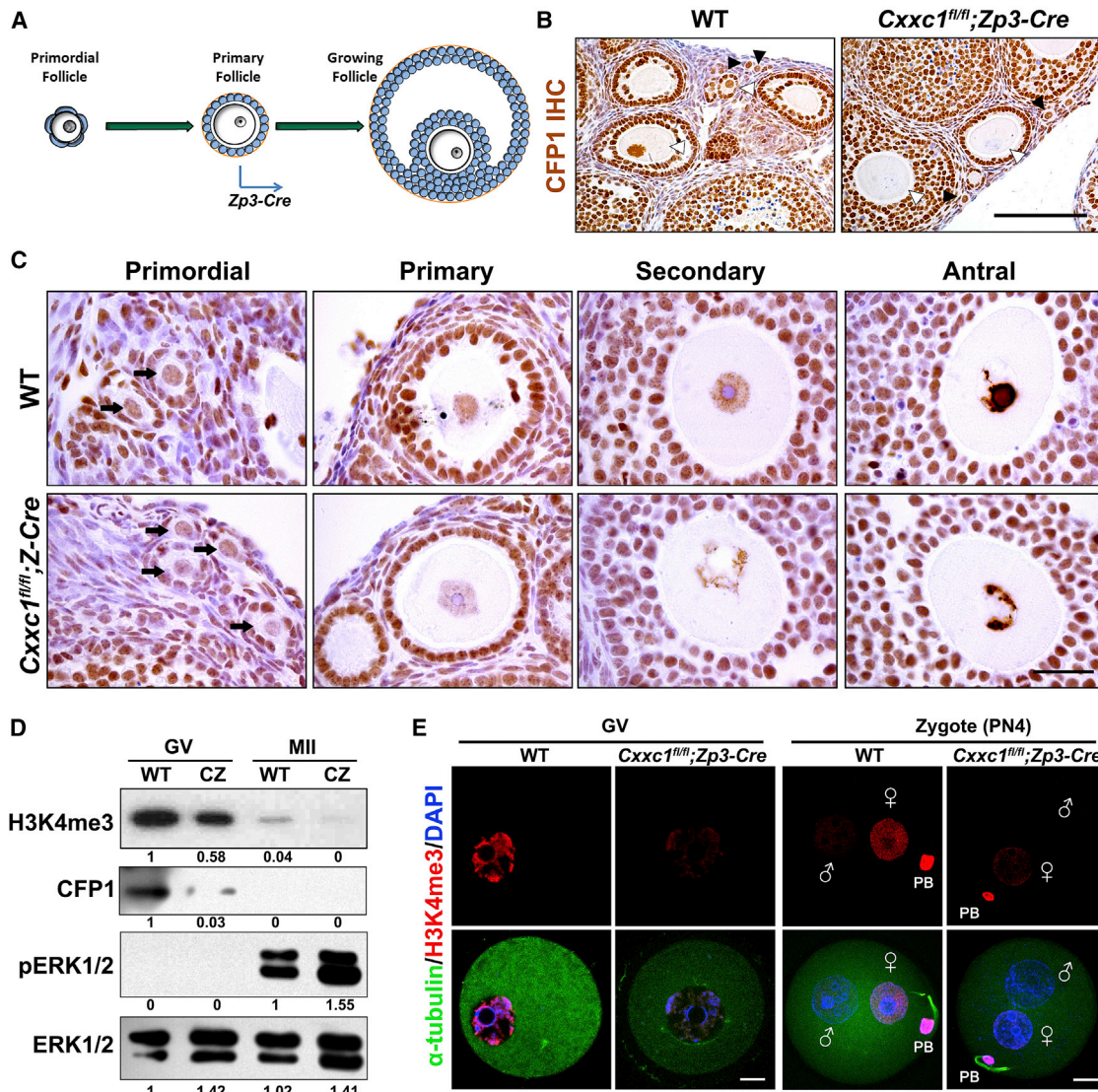


**Figure 1. Maternal CFP1 Deletion Leads to a Decrease of H3K4me3 in Mouse Oocytes and Zygotes**

(A) Illustration of *Zp3-Cre*-mediated *Cxxc1* knockout in oocytes of growing follicles.

(B) Immunohistochemistry (IHC) staining of CFP1 in ovaries of WT and *Cxxc1<sup>fl/fl</sup>;Zp3-Cre* mice (3-week-old). Black and white arrowheads indicate primordial and activated follicles, respectively. Scale bar, 100  $\mu$ m.

(C) IHC results showing the H3K4me3 level in the oocytes of WT and *Cxxc1<sup>fl/fl</sup>;Zp3-Cre* mice. The stages of follicles are indicated. Arrows indicate oocytes within primordial follicles. Scale bar, 30  $\mu$ m. For each genotype, at least five females were used. Z-Cre is short for *Zp3-Cre*.

(D) Western blot analysis showing H3K4me3 levels in WT and CFP1-deleted oocytes at GV (germinal vesicle) and MII (metaphase II) stages. Quantification results are provided below the blots. ERK1/2 was blotted as a loading control, and phosphorylated ERK1/2 (pERK1/2) was blotted to indicate MII arrest. Total proteins from 100 oocytes were loaded in each lane. CZ is short for *Cxxc1<sup>fl/fl</sup>;Zp3-Cre*.

(E) Immunofluorescence (IF) showing levels of H3K4me3 (red) in GV oocytes and pronuclear stage 4 (PN4) zygotes of WT and *Cxxc1<sup>fl/fl</sup>;Zp3-Cre* mice.  $\alpha$ -tubulin and 4',6'-diamidino-2-phenylindole (DAPI) were co-stained to show the morphology. Female and male symbols indicate the female and male pronuclei, respectively. PB, polar body. More than ten oocytes or zygotes of each genotype were observed with similar results. Scale bar, 20  $\mu$ m.

results (ERCC evaluated absolute copy number) and shown in Figure 3E.

To investigate the age-dependent changes of the oocyte transcriptome after CFP1 deletion, we analyzed CFP1-deleted oocytes (oocytes from *Cxxc1<sup>fl/fl</sup>;Gdf9-Cre* females) at the age of 3 months (Figures 3F and 3G). The total mRNA copy numbers in these oocytes exhibited 60% decrease when compared to WT

control (Figure 3F). When compared with the WT oocytes, 770 genes were significantly downregulated in the CFP1-deleted oocytes (Figure 3G). The expression levels of these genes were lower than normal in the CFP1-deleted oocytes isolated from both 3-week-old and 3-month-old females (Figure 3G). These results indicate that CFP1 deletion causes gene expression defects in oocytes of both pubertal and adult mice.

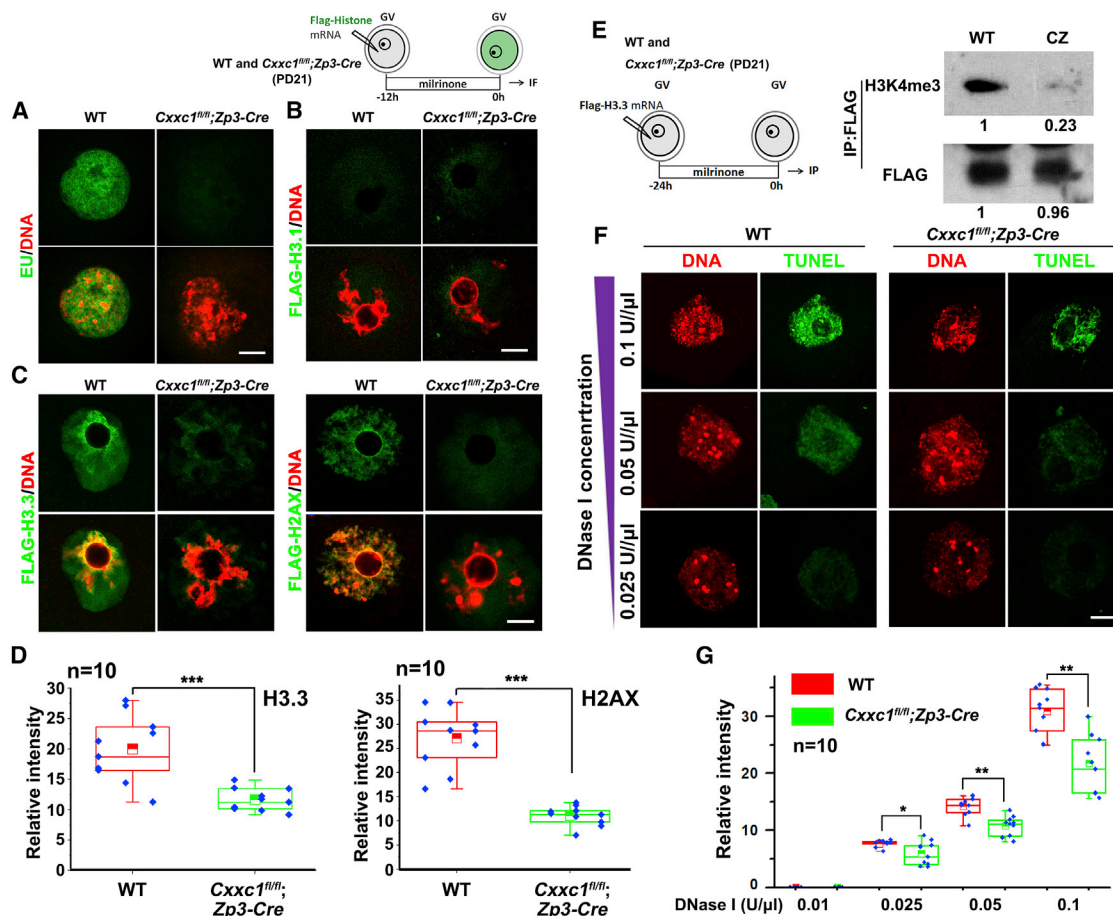


**Figure 2. Effect of CFP1 Deletion on Oocyte Transcriptional Activity and Chromatin Accessibility**

(A) Detection of newly synthesized RNA by EU incorporation in growing WT and CFP1-deleted oocytes. More than ten oocytes of each genotype were observed with similar results. Scale bar, 10 μm for all panels.

(B and C) WT and *Cxhc1<sup>tm</sup>;Zp3-Cre* oocytes were subjected to mRNA microinjection of FLAG-tagged histone H3.1 (B), H3.3, or H2AX (C). Incorporation of histone variants was visualized by anti-FLAG antibody staining.

(D) Quantification of FLAG-histone H3.3 and H2AX signal intensity in GV of WT and *Cxhc1<sup>tm</sup>;Zp3-Cre* oocytes. n = 10 for each treated group. Error bars, SEM. \*\*\*p < 0.001 by two-tailed Student's t tests.

(E) FLAG-histone H3.3 was immunoprecipitated from 130 WT or *Cxhc1<sup>tm</sup>;Zp3-Cre* oocytes after microinjection and subjected to western blotting of H3K4me3.

(F) DNase I-TUNEL assay in WT and *Cxhc1<sup>tm</sup>;Zp3-Cre* oocytes showing accessibility of genomic DNA to DNase I.

(G) Quantification of TUNEL signal intensity in GV of WT and *Cxhc1<sup>tm</sup>;Zp3-Cre* oocytes after DNase I digestion. n = 10 for each treated group. Error bars, SEM. \*\*p < 0.01 and \*p < 0.05 by two-tailed Student's t tests.

### CFP1 Deletion Indirectly Impaired Maternal mRNA Clearance

We categorized genes as three clusters (GV-zygote increased, GV-zygote decreased, and GV-zygote stable) according to their expression pattern from the WT GV oocytes to WT zygotes and compared the results calculated by FPKM and absolute mRNA copy number evaluated by ERCC spike-ins (Figure S4B). There were more differentially expressed genes found by the calculation using absolute copy numbers, indicating that this approach was more sensitive.

The GV-zygote decreased genes were maternal transcripts that are degraded after fertilization. As shown by gene set enrichment assay (GSEA), these genes were more enriched in the WT samples at the GV stage (Figure 3H, left) but showed obvious enrichment in the CFP1-deleted samples at the zygote stage

(Figure 3H, right). These results suggested that CFP1 is important for both maternal RNA synthesis and degradation. Based on the divided gene categories (Figure S4B), GV-zygote decreased genes failed to be degraded in zygotes after CFP1 deletion (Figure 3H). We divided these maternal genes into five expression bins according to their expression levels in WT GV oocytes. These genes were degraded from the GV to zygote transitions, but the degradation was largely blocked by CFP1 deletion (Figure 3I).

To investigate the molecular bases of maternal *Cxhc1* knockout-mediated zygotic developmental arrest, we analyzed the influence of CFP1 deletion on the transcriptome during maternal-zygotic transition. According to the principal components analysis, the transcriptomes of WT and CFP1-deleted embryos at the zygote stage were strikingly different (Figure 3A).

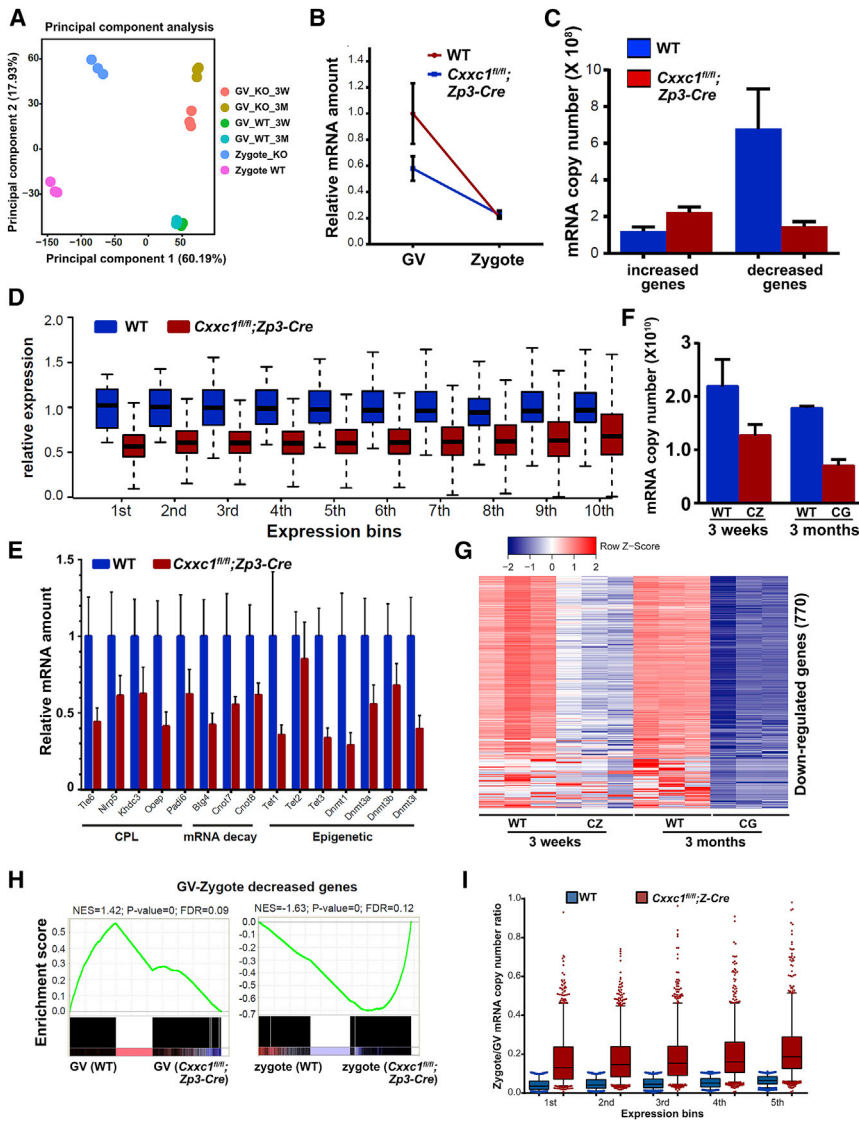


**Figure 3. Transcriptome Changes in CFP1-Deleted Oocytes and Zygotes**

(A) Principal component analysis (PCA) results showing the differences among different stages of GV oocytes and zygotes (both WT and CFP1 depleted). (B) Changes of relative mRNA copy numbers in WT and maternal CFP1-deleted samples at different stages. Error bars indicate SEM for all panels. (C) Evaluation of mRNA abundance regarding to the increased genes and decreased genes in the CFP1-depleted GV oocyte samples. There were 5,588 increased genes and 3,103 decreased genes by setting the criteria of  $\log_2$  (fold change [GV\_CZ/GV\_WT])  $>0.5$  or  $<-0.5$ , with the p value  $<0.05$ , false discovery rate [FDR]  $<0.05$ . (D) Relative mRNA amount of WT and CFP1-deleted GV oocytes in each bin. There were 12,521 genes showed expressions in GV\_WT oocytes. These genes were divided into ten equal size bins according to their average expression levels in the GV\_WT oocytes. (E) Relative expression of selected genes extracted from RNA-seq data. (F) Total mRNA copy numbers evaluated by ERCC in 60 WT and CFP1-deleted oocytes at indicated ages. CZ stands for *Cxhc1<sup>fl/fl</sup>;Zp3-Cre* while CG stands for *Cxhc1<sup>fl/fl</sup>;Gdf9-Cre*. (G) Heatmap of genes found to be downregulated using absolute mRNA analysis at the 3-week and 3-month old GV oocytes after CFP1 depletion. (H) Gene set enrichment analysis (GSEA) results using genes that decreased from GV to zygotic stage (Figure S4B). The enrichment are considered significant when the FDR  $<0.25$ . NES, normalized enrichment score. (I) Ratio of mRNA copy numbers in zygotes versus GV oocytes indicates defects of maternal mRNA degradation in CFP1-deleted zygotes. Error bars, SEM.

Maternal transcripts of *Btg4*, *Cnot7*, and *Cnot8*, which are involved in the bulk degradation of maternal mRNA upon fertilization (Liu et al., 2016b; Yu et al., 2016), were downregulated in the CFP1-deleted oocytes (Figure 3E). Western blot results also showed that the expression of BTG4, the licensing factor of maternal mRNA clearance in mammals, was impaired in the CFP1-deleted MII oocytes (Figure 4A). Relative mRNA levels of representative maternal genes are extracted from RNA-seq results (Figure 4B). These results indicate that CFP1 is crucial for the accumulation of maternal factors that control maternal-zygotic transition.

### Maternal CFP1 Deletion Causes Early Developmental Arrest after Fertilization

To determine the developmental potential of CFP1-deleted oocytes after fertilization, *Cxhc1<sup>fl/fl</sup>;Zp3-Cre* female mice were superovulated and mated with WT males. The CFP1-deleted

oocytes were fertilized normally, but none of the embryos derived from these oocytes developed beyond the 2-cell stage (Figures 4C–4E). These maternal CFP1-deleted embryos (arrested at the 1–2-cell stage) exhibited severe defects in zygotic genome activation, as shown by immunofluorescence staining of RNA polymerase II phosphorylation (pS2) and mRNA synthesis-coupled EU incorporation assay (Figures 4F, 4G, and S5C).

To compare the distinct contributions of maternal-versus zygotic-derived CFP1 to preimplantation development, we also generated zygotic *Cxhc1* knockout (*Cxhc1<sup>-/-</sup>*) embryos by crossing *Cxhc1<sup>+/-</sup>* females with *Cxhc1<sup>+/-</sup>* males (Figure S5A). We did not detect any nuclear-localized CFP1 signal in the *Cxhc1<sup>-/-</sup>* embryos, indicating that they are truly null for *Cxhc1*, but these embryos were able to develop to the morula and blastocyst stages (Figure S5B). This observation is consistent with previous reports (Carlone and Skalnik, 2001) and indicates that the expression of zygotic CFP1, if any (Figures S2B and S2C), is not required for preimplantation

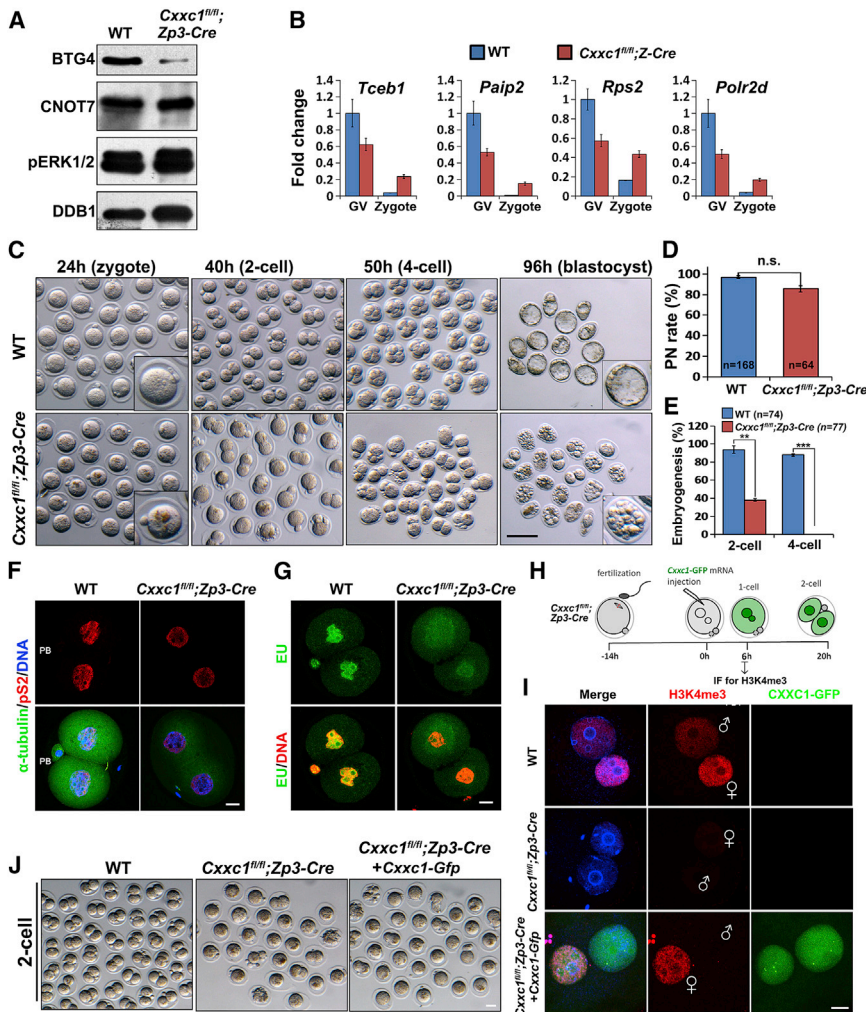


**Figure 4. Maternal Deletion of CFP1 in Oocytes Caused Zygote to 2-Cell Arrest after Fertilization and Defects in Maternal mRNA Decay**

(A) Western blot showing the expression of BTG4 and CNOT7 in 100 WT and CFP1-deleted MII oocytes. DDB1 was blotted as a loading control.

(B) Relative mRNA levels of selected maternal transcripts extracted from RNA-seq results. Error bars, SEM.

(C) Representative images of embryos derived from WT and *Cxhc1<sup>fl/fl</sup>;Zp3-Cre* females. *n* = 5 mice for each genotype at each developmental stage. Scale bar, 100  $\mu$ m.

(D) Statistic analysis of pronucleus (PN) formation in WT and *Cxhc1<sup>fl/fl</sup>;Zp3-Cre* oocytes after fertilization. Error bars, SEM. n.s., not significant. *n* indicates numbers of embryos analyzed.

(E) Developmental rates of maternal CFP1-deleted embryos at the time when WT embryos reached corresponding stages. *n* indicates numbers of embryos analyzed. Error bars, SEM. \*\**p* < 0.01 and \*\*\**p* < 0.001 by two-tailed Student's *t* tests.

(F and G) Immunofluorescent staining of phosphorylated RNA polymerase II CTD repeat YSPTSPS (pS2) (F) and EU staining (G) showing the zygotic genome activation in 2-cell embryos derived from WT and *Cxhc1<sup>fl/fl</sup>;Zp3-Cre* females mated with WT males. For each genotype, at least 15 embryos were observed with similar results. Scale bar, 10  $\mu$ m.

(H–J) (H) Illustration of mRNA microinjection and sample collection in (I) and (J). (I) Expression of CFP1-GFP and levels of H3K4me3 in zygotes derived from *Cxhc1<sup>fl/fl</sup>;Zp3-Cre* females at 6 hr after mRNA microinjection (bottom panels). Non-injected zygotes derived from WT and *Cxhc1<sup>fl/fl</sup>;Zp3-Cre* females were imaged as controls (top and middle panels). Zygotes are analyzed at PN4–5 stages. Scale bar, 50  $\mu$ m.

(J) Zygotes collected from *Cxhc1<sup>fl/fl</sup>;Zp3-Cre* females were injected with mRNAs encoding for *Cxhc1*-GFP, and were further cultured for 20 hr. Non-injected zygotes derived from WT and *Cxhc1<sup>fl/fl</sup>;Zp3-Cre* females were imaged as controls. More than 30 embryos were observed in each experimental group with similar results. Scale bar, 50  $\mu$ m.

embryogenesis, which is different from the maternal CFP1 deletion in growing oocytes.

In addition, we performed a rescue experiment by injecting the mRNA encoding CFP1-GFP into the fertilized eggs derived from CFP1-deleted oocytes (Figure 4H). CFP1-GFP was translated by the injected mRNAs and localized in both male and female pronuclei (Figure 4I). Interestingly, H3K4me3 levels were only restored in female but not male pronucleus (Figure 4I, bottom panels; Figure S5D). This preferential H3K4 trimethylation in female pronucleus mimicked the asymmetrical H3K4me3 distribution pattern in WT zygotes (Figure 4I, top panels). However, when the WT zygotes developed into the 2-cell stage after microinjection, the zygotically translated CFP1 failed to rescue the developmental arrest caused by maternal *Cxhc1* knockout (Figure 4J). These results further indicate that maternal CFP1, but not *de novo* synthesized zygotic CFP1, is crucial for early embryo development beyond the 1–2-cell stage.

### CFP1 Regulates the Dynamics of Cytoskeleton in Oocytes

Morphologically, the CFP1-deleted oocytes contained aggregated, brown cytoplasmic granules (Figure 5A). These granules were apparent in oocytes of 3-week-old mice but were more remarkable at 3 months of age. Transmission electron microscopy (TEM) results showed that these cytoplasmic granules were aggregates of lipid droplets and other organelles (Figures 5B and S6A). Nile red staining results showed that the lipid droplets were more aggregated in the CFP1-deleted oocytes and zygotes than in the WT controls (Figure 5C). CFP1 deletion also altered the normal distribution of mitochondria in the oocyte and caused their aggregation, as shown by the TEM results (Figures 5B and S6A) and immunofluorescence staining of the mitochondrial protein HSP60 (Figure 5D). Moreover, other organelles, including the Golgi apparatus, endoplasmic reticulum, and cortex granules, marked by GM130, calnexin, and Con-A, respectively, were also abnormally aggregated in the

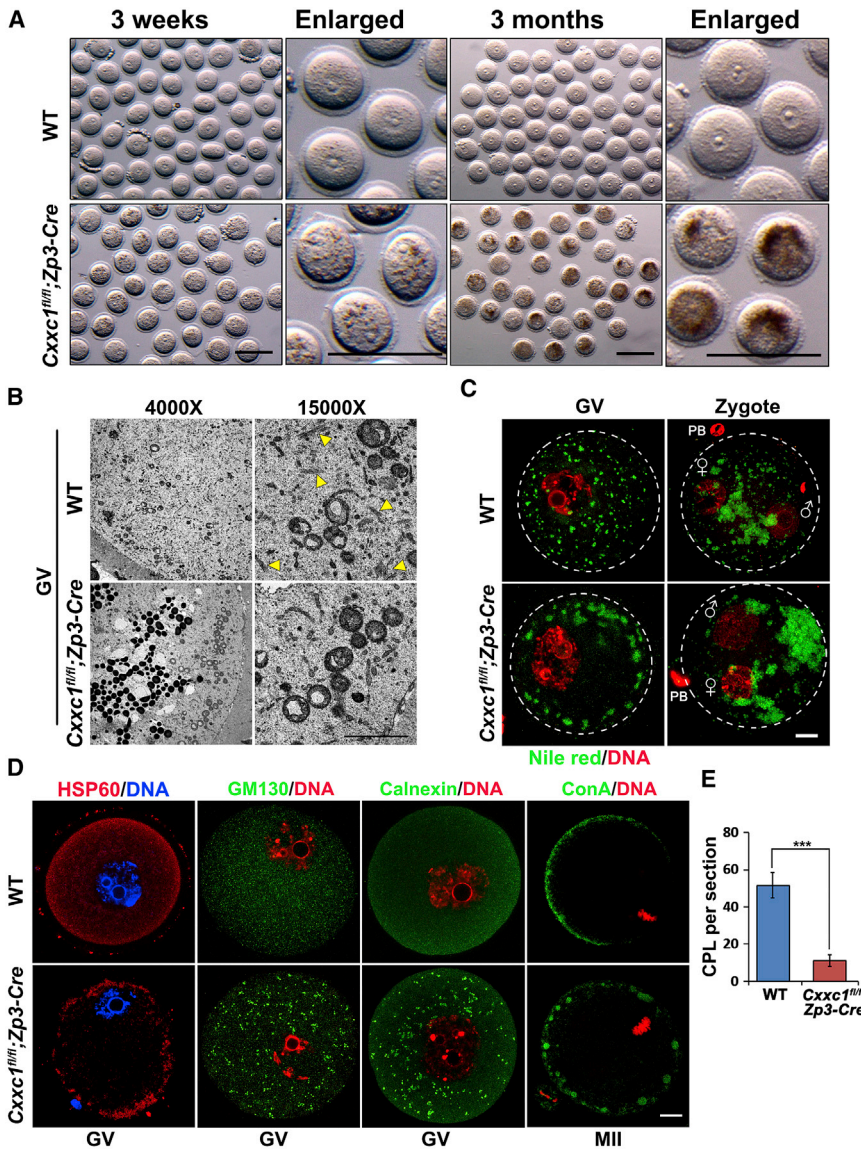


**Figure 5. CFP1 Is Crucial for Proper Cytoplasmic Organelle Distributions and Assembly of Subcortical Maternal Complex in Oocytes**

(A) Representative images of GV stage oocytes derived from 3-week and 3-month old WT and *Cxxc1<sup>fl/fl</sup>;Zp3-Cre* females. *n* = 6 mice for each genotype at each developmental stage. Scale bar, 100  $\mu$ m.

(B) Transmission electron microscopy (TEM) results of WT and CFP1-deleted oocytes at GV stages. Arrowheads indicate cytoplasmic lattices (CPLs). Scale bars, 2  $\mu$ m.

(C) Nile red staining showing the distribution of lipid droplets in WT and CFP1-deleted oocytes and zygotes. For each genotype, at least 15 oocytes or embryos were observed with similar results. Scale bars, 10  $\mu$ m.

(D) Distributions of HSP60 (mitochondrial marker), GM130 (Golgi marker), Calnexin (endoplasmic reticulum marker), and Con-A (cortical granule marker), in WT and CFP1-deleted oocytes. For each genotype, at least 15 oocytes or embryos were observed with similar results. Scale bars, 10  $\mu$ m.

(E) Statistical analysis showing the numbers of cytoplasmic lattices in WT and CFP1-deleted oocytes in 15,000 $\times$  TEM pictures. Error bars, SEM. \*\*\**p* < 0.001 by two-tailed Student's *t* tests.

CFP1-deleted oocytes (Figure 5D). However, in *Cxxc1* knockout HeLa cells, the distribution of these organelles was not affected (Figures S6B and S6C). These results indicate that CFP1 deletion disrupts normal organelle distribution specifically in oocytes.

The subcortical maternal complex (SCMC) is essential for the distribution of cytoplasmic organelles and the first cell division after fertilization (Li et al., 2008). The SCMC contains MATER (encoded by *Nlrp5*), FILIA (encoded by *Khdc3*), FLOPED (encoded by *Ooep*), TLE6, and PADI6. These proteins are crucial for the formation of a unique oocyte cytoplasmic structure named the cytoplasmic lattice (CPL). Cytoplasmic lattice assembly is a hallmark of oocyte cytoplasmic maturation. Deletion of genes encoding cytoplasmic lattice components caused aggregation of cytoplasmic organelles and 2-cell arrest after fertilization (Kim et al., 2010, 2014; Li et al., 2013; Tashiro et al., 2010). TEM results showed that the number of cytoplasmic lattices

was significantly decreased after CFP1 deletion (Figures 5B and 5E). From the RNA-seq results, we also observed a downregulation of cytoplasmic lattice-related genes in the CFP1-deleted oocytes (Figure 3E). These results suggest that CFP1 ensures the expression of cytoplasmic lattice-related genes to affect cytoplasmic lattice assembly and organelle distribution in oocytes.

In PADI6-deleted oocytes, tubulin polymerization is disrupted, suggesting that cytoplasmic lattices are required for this process (Kim et al., 2014). CFP1 deletion had no effect on  $\alpha$ -tubulin expression (Figure 6A). However, after Triton X-100 extraction, there were fewer polymerized  $\alpha$ -tubulin molecules left in the CFP1-deleted oocytes than in WT oocytes (Figures 6A and 6B). Upon meiotic resumption, tubulins are polymerized to assemble the meiotic spindle. Therefore, we analyzed the meiotic maturation process of CFP1-deleted oocytes. After superovulation, the CFP1-deleted oocytes were able to undergo GV breakdown, emit the polar body 1 (PB1), and develop to the MII stage (Figures 6C and 6D). However, CFP1-deleted oocytes failed to assemble bivalent MII spindles, suggesting that CFP1 regulates  $\alpha$ -tubulin polymerization in oocytes (Figure 6D). CFP1 deletion also caused aneuploidy in meiosis II, as determined from the number of separating sister chromatids counted after *in vitro* fertilization (Figures 6E and 6F). However, the PB1 emission rates were not affected in oocytes of *Cxxc1<sup>fl/fl</sup>;Zp3-Cre* mice (Figure 6G). These results indicate that CFP1-mediated maternal

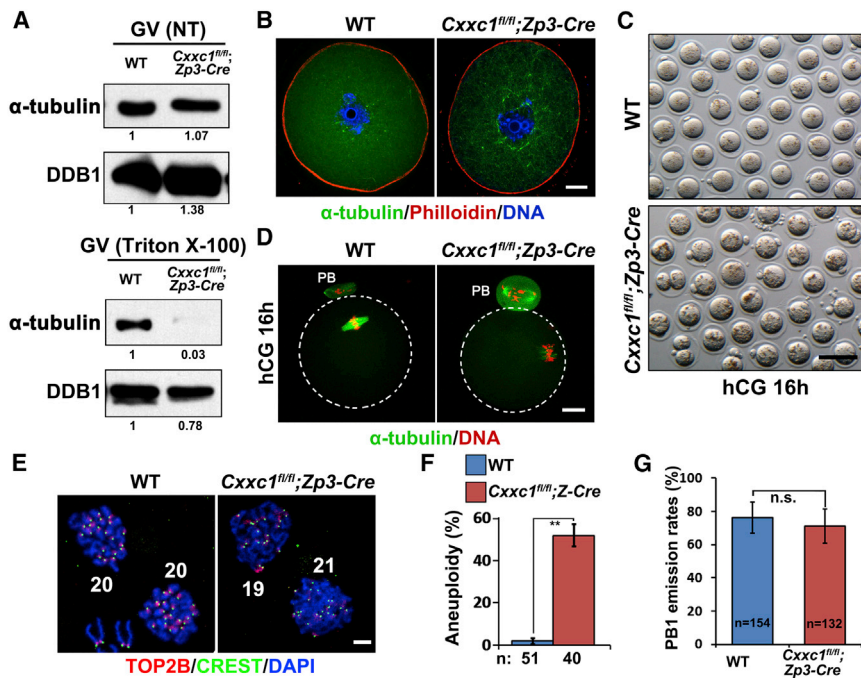


**Figure 6. Deletion of CFP1 in Oocytes Caused Defects in  $\alpha$ -Tubulin Polymerization and Aneuploidy in Meiosis**

(A) Western blot results showing total and polymerized  $\alpha$ -tubulin in WT and CFP1-deleted oocytes. Protein lysates from 100 oocytes were loaded in each lane. DDB1 was blotted as a loading control. (B) Immunofluorescence staining results showing  $\alpha$ -tubulin (green) and actin (red) polymerization in WT and CFP1-deleted oocytes.  $\alpha$ -tubulin was labeled by a fluorescein isothiocyanate (FITC)-conjugated antibody, and polymerized actin microfilaments were labeled by phalloidin. Scale bar, 10  $\mu$ m. For each genotype, at least 15 oocytes were observed with similar results. (C and D) Morphology (C) and spindle formation (D) of MII oocytes derived from WT and *Cxhc1<sup>fl/fl</sup>;Zp3-Cre* females. Scale bar, 100  $\mu$ m. n = 8 mice for each genotype. (E and F) Chromosome spread results (E) showing the rates of aneuploidy (F) in WT and CFP1-deleted oocytes during meiosis II. Error bars, SEM n indicates numbers of oocytes analyzed. \*\*p < 0.01 by two-tailed Student's t tests. (G) Quantified PB1 emission rates in WT and CFP1-deleted GV oocytes at 14 hr after *in vitro* culture. Error bars, SEM n indicates numbers of oocytes analyzed. n.s. p > 0.05 by two-tailed Student's t tests.

epigenetic changes contribute to proper spindle assembly and precise chromosome separation during oocyte meiosis.

### CFP1 Deletion Causes Defects in DNA Methylation and Demethylation in Oocytes and Zygotes, Respectively

During follicle growth, the oocyte genome is methylated and acquires the maternal imprints. CFP1-mediated H3K4 methylation was reported to be important for maintaining DNA methylation levels in ESCs (Butler et al., 2008). Therefore, we investigated the effect of CFP1 deletion on the establishment of DNA methylation. GV oocytes were collected from WT and *Cxhc1<sup>fl/fl</sup>;Zp3-Cre* females and subjected to immunofluorescence staining of 5'-methylcytosine (5mC). As shown in Figure 7A, the global DNA methylation level was decreased in the CFP1-deleted oocytes at both NSN and SN stages, indicating that CFP1 particularly affects the establishment of maternal DNA methylation. Notably, the DNA methyltransferases (DNMTs) required for DNA methylation, including *Dnmt1*, *Dnmt3a/b*, and *Dnmt3l*, were all downregulated in the CFP1-deleted oocytes (Figure 3E). Particularly, *Dnmt3a* and *Dnmt3l* belong to the functionally critical machinery that is involved in *de novo* re-establishment of the oocytes methylation landscape. These results indicate that CFP1 deletion in oocytes impairs the expression of DNMTs, and causes defects of *de novo* DNA methylation.

In zygotes, maternal TET3 converts the 5mC to 5'-hydroxymethylcytosine (5hmC) for DNA demethylation, which is crucial for the developmental competence of embryos (Gu et al., 2011). In the CFP1-deleted zygotes, *Tet3* mRNA was downregulated (Figure 3E), and the 5mC to 5hmC transition was blocked, particularly in the male pronucleus (Figure 7B). Consistent with this observation, phosphorylated histone H2AX, a marker of genome reprogramming-induced DNA strand breaks (Hajkova et al.,

2010), was clearly present in pronuclei of the WT zygotes (with more dotted signals in male pronuclei than in female pronuclei) but was not detected in the CFP1-deleted zygotes (Figures 7C and S5E). These results demonstrate that, by affecting H3K4 trimethylation, CFP1 regulates the transcription of other maternal epigenetic regulators during oocyte growth and renders developmental competence of the oocytes.

### DISCUSSION

In this study, we identified CFP1 as a key regulator of histone modification maturation in oocytes (Figure 7D). The H3K4me3 level was low in growing oocytes, but high in fully grown oocytes, indicating that H3K4me3 is a marker of epigenetic maturation. Defective H3K4 trimethylation by *Cxhc1* knockout impaired the exchanges of histone variants, reduced the genome accessibility, and decreased the global transcription activity in growing oocytes, which were devoid of proliferation and DNA replication. Therefore, our observations in this unique *in vivo* system demonstrate an essential role of CFP1-mediated H3K4 trimethylation in maintaining a dynamic chromatin structure and normal transcriptomes in highly differentiated, post-proliferative cells.

In mammalian cells, H3K4 trimethylation is mediated mainly by the SETD1 complex and mixed-lineage leukemia (MLL) family of proteins (Long et al., 2013). H3K4me3 levels were markedly decreased, but not completely abolished, in CFP1-deleted oocytes. This indicates the involvement of other H3K4 methyltransferases in oocyte development. A previous study suggested that MLL2 also contributes to H3K4 trimethylation in oocytes (Andreu-Vieyra et al., 2010). Similar to CFP1 deletion, MLL2 deletion in oocytes led to a decrease of H3K4me3 levels and female infertility.

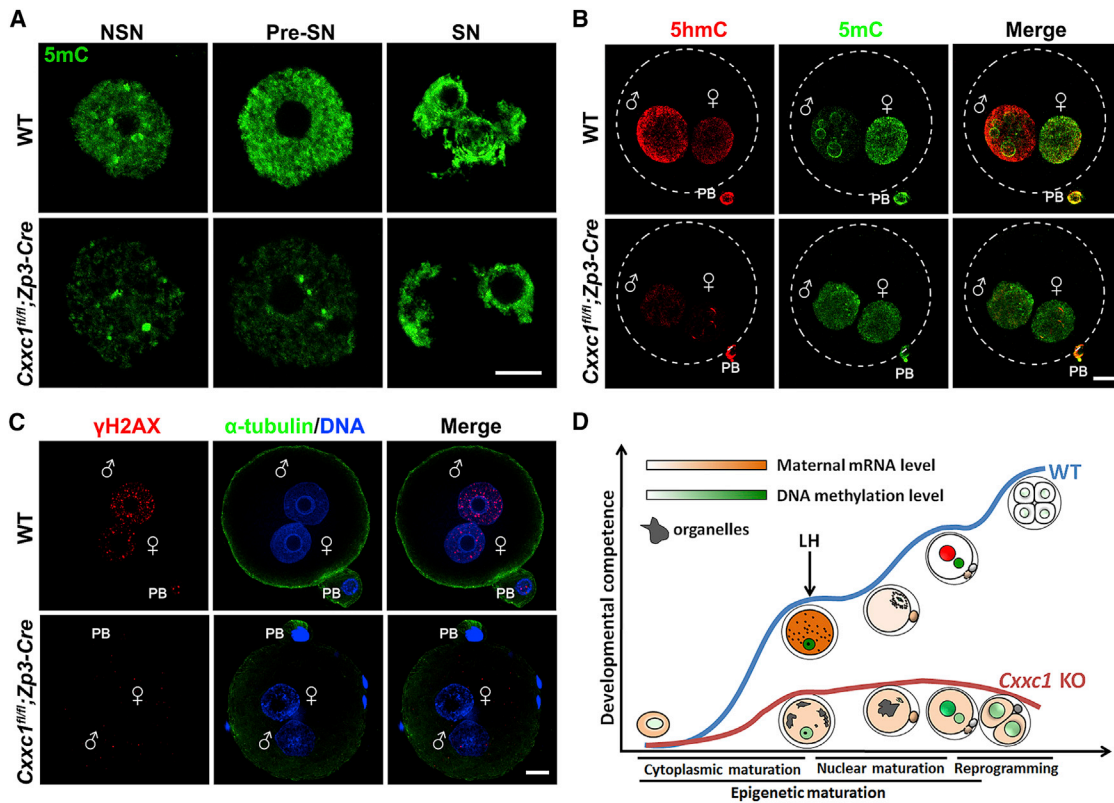


**Figure 7. DNA Methylation and/or Demethylation Defects in CFP1-Deleted Oocytes and Zygotes**

(A) Immunofluorescent staining of 5'-methylcytosine (5mC) showing the DNA methylation status in nuclei of WT and CFP1-deleted oocytes. For each stage, at least 15 oocytes were observed with similar results. Scale bar, 10  $\mu$ m.

(B) Immunofluorescent staining of 5'-hydroxymethylcytosine (5hmC) and 5mC showing the reprogramming of paternal DNA in PN4–5 zygotes derived from WT and CFP1-deleted oocytes. For each stage, at least 15 oocytes were used. Scale bar, 10  $\mu$ m.

(C) Immunofluorescent staining of phosphorylated histone H2AX (pH2AX) showing the status of DNA damage in WT and maternal CFP1-deleted zygotes (PN4). Error bar, 10  $\mu$ m.

(D) Summary of CFP1 functions in epigenetic maturation and developmental competence acquisition of oocytes. Besides cytoplasmic maturation that prepare energy and materials and nuclear maturation that give rise to precise chromosome sets, oocytes experienced epigenetic maturation during oogenesis, including methylation of genomic DNA and establishment of the histone modifications. CFP1 deletion in oocytes decreased histone H3K4 trimethylation and caused global downregulation of maternal genes. These genes are involved in cytoplasmic lattice formation, maternal-zygotic transition, and DNA methylation and/or demethylation. CFP1-deleted oocytes fail to complete epigenetic maturation and unable to gain developmental competence during oogenesis.

CFP1 deletion affected the expression of a wide range of maternal genes, disregarding their original expression abundances. Insufficient H3K4 trimethylation and decreased genome transcription impaired the acquisition of oocyte competence. Previous studies have shown that CFP1 deletion in mouse ESCs leads to a marked loss of H3K4me3 at CGI-associated genes but did not affect the transcriptomes (Clouaire et al., 2014). Therefore, CFP1 plays a poising, rather than a house-keeping role in somatic cells, by facilitating gene expression in an environment- and cell-type-specific manner. However, our study emphasizes the requirements of CFP1-mediated H3K4me3 generation in maintaining essential genome transcriptional activity during oogenesis.

A group of maternal transcripts that depend on CFP1 for expression are those that encode cytoplasmic lattice components. Cytoplasmic lattices are unique cytoskeleton structures in oocytes that are essential for ooplasm compartmentation and zygotic cytokinesis. The oocyte is an extraordinarily large

cell and contains significantly more organelles (including mitochondria, lipid droplets, and Golgi apparatus) than those in somatic cells. Therefore, it is crucial for oocytes to maintain these organelles in their proper subcellular locations and to prevent their abnormal aggregation. However, it was previously unclear how the cytoplasmic lattice network is established and what mechanism ensures the active expression of cytoplasmic lattice components in oocytes. In this study, we provide evidence that CFP1-mediated epigenetic regulation of the oocyte genome is essential for the expression of cytoplasmic lattice components and proper distribution of organelles. The role of CFP1 in affecting organelle distribution appears to be oocyte-specific, because the subcellular localizations of organelles remained normal in *Cxxc1* knockout HeLa cells.

A balanced H3K4 methylation status is essential not only for maintaining transcription in the growing oocyte, but also for triggering zygotic genome activation. Histone H3K4me3 is enriched in female pronucleus after fertilization and is only begun to be

detected in male pronucleus at the late zygotic stage (Lepikhov and Walter, 2004). In developing oocytes and zygotes, MLL2, MLL3, and MLL4 were being reported to contribute to H3K4 methylation (Andreu-Vieyra et al., 2010; Aoshima et al., 2015), whereas KDM1A, KDM1B, and KDM5B were reported to demethylate H3K4 (Dahl et al., 2016; Zhang et al., 2016). Deletion of these lysine demethylases (KDMs) caused defects in oogenesis and zygotic genome activation (Ancelin et al., 2016; Ciccone et al., 2009; Kim et al., 2015; Wasson et al., 2016). Based on these observations and recent chromatin immunoprecipitation sequencing (ChIP-seq) studies, the role of H3K4 demethylation in establishing the maternal chromatin and transcription landscapes has been recognized (Dahl et al., 2016; Liu et al., 2016a). H3K4me3 deposits gene promoters as broad peaks on oocyte genome but is promptly removed by KDMs after fertilization. As a result, only narrow and sharp H3K4me3 peaks remained on the genome of 2- to 4-cell embryos. This large-scale H3K4me3 removal from maternal genome is necessary for successful zygotic genome activation. We also observed a transient drop of H3K4me3 levels in 2–4-cell embryos, which coincided with the downregulation of CFP1. Nevertheless, results of this study and other reports indicated that insufficient maternal H3K4me3 accumulation also caused failure of preimplantation embryonic development: maternal *Mll2* knockout embryos arrest at the 2-cell stage (Andreu-Vieyra et al., 2010); inhibition of histone H3K4 methyltransferase activity by overexpressing a dominant-negative histone H3 mutant (K4-to-M mutation) in oocytes also blocked zygotic genome activation and impaired embryonic development (Aoshima et al., 2015).

These studies of H3K4me3 functions in zygotic genome activation are not contradictory: although the removal of bulk H3K4me3 from zygotic chromatin is a key step that leads to zygotic genome activation, the proper deposition of H3K4me3 at the promoters of certain important zygotic genes (as narrow peaks) are also required; CFP2-dependent H3K4 trimethylation is involved in the fine-tune regulation of gene expression at different developmental stages. For example, both H3K4me3 and CFP1 nuclear localization were restored after the 8-cell stage, coinciding with the first lineage commitment in early embryos. Collectively, these results suggest that the balanced H3K4 modification mediated by both CFP1 and KDMs is crucial for the acquisition of oocyte competence.

The maternal CFP1-deleted embryo was arrested at the zygote to 2-cell stages, suggesting that CFP1 has stronger impacts on their developmental competence in several ways. In zygotes derived from CFP1-deleted oocytes, maternal mRNAs failed to be degraded. We recently identified the maternal factor BTG4 as an maternal-zygotic transition licensing factor (Yu et al., 2016). BTG4 recruits the RNA deadenylases CNOT7 and CNOT8 to facilitate maternal mRNA decay (Liu et al., 2016b; Wu and Dean, 2016). The transcription of all these genes was decreased in CFP1-deleted oocytes. It appears that the maternal CFP1 plays a key role in determining zygotic developmental competence, because *de novo* translated CFP1 protein in maternal CFP1-deleted zygotes failed to rescue the zygotic genome activation defects.

Taken together, the results indicate that CFP1 maintains H3K4me3 and the transcription of bulk maternal mRNAs in

oocytes, providing them with high developmental competence after fertilization. Our studies also provide insight into the histone dynamic *in vivo* and highlight the importance of studying chromatin in a physiological context and in non-proliferating post-mitotic cells.

## EXPERIMENTAL PROCEDURES

### Mice

All mice used were handled with care and according to the Animal Research Committee guidelines of Zhejiang University. *Cxhc1<sup>fl/fl</sup>* mouse strain has been engineered and described previously (Cao et al., 2016). *Zp3-Cre* transgenic mice were previously reported (Lewandoski et al., 1997). All mice have a C57BL/6J genetic background. Primers used for genotyping are listed in Table S2. Sample size, gender, and age in each experiment were indicated in related figure legends.

### Embryo Collection and Culture

Mice were superovulated and fertilized by WT males and checked for the presence of vaginal plugs. E0.5 embryos (zygotes) were collected from the oviducts and released into a hyaluronidase/M2 solution for dissociation. E1.5 (2-cell) embryos were flushed out of the oviducts, and E3.5 embryos (blastocysts) were flushed out of the uteri. In some experiments the obtained embryos were further cultured at 37°C, 5% CO<sub>2</sub> in KSOM (Millipore).

### Immunofluorescent Staining

Oocytes were fixed in 4% paraformaldehyde in PBS for 30 min and permeabilized for 15 min in 0.2% Triton X-100 in PBS. For oocytes microinjected with mRNAs encoding FLAG-tagged histones, they were pre-extracted with 0.1% Triton X-100 for 5 min before fixation. Antibody staining was performed using standard protocols described previously (Yu et al., 2015). The antibodies used are listed in Table S3. Imaging of embryos following immunofluorescence was performed on a Zeiss LSM710 confocal microscope.

### In Vitro mRNA Synthesis and Microinjection

*In vitro* mRNA synthesis and microinjections were performed as described previously (Yu et al., 2016). Microinjection was performed under an inverted microscope (Eclipse TE200; Nikon) using micromanipulator and microinjector (Eppendorf). Approximately 10 pl synthetic RNA (~200 µg/mL) was microinjected into the cytoplasm of oocytes or zygotes.

### Histological Analysis

Ovaries were collected and fixed in formalin overnight, processed, and embedded in paraffin using standard protocols. Ovaries were serially sectioned at 5 µm and stained with H&E. IHC was performed using standard protocols. The antibodies used are listed in Table S3.

### Western Blotting

100 oocytes or embryos were lysed in 2-mercaptoethanol containing loading buffer and heated at 95°C for 5 min. SDS-PAGE and immunoblots were performed following standard procedures using a Mini-PROTEAN Tetra Cell System (Bio-Rad). The antibodies used are listed in Table S3.

### Real-Time RT-PCR

Total RNA was extracted from oocytes using the RNeasy Mini kit (QIAGEN) according to the manufacturer's instruction, followed by RT using Superscript RT kit (Bio-Rad). qRT-PCR was performed using a Power SYBR Green PCR Master Mix (Applied Biosystems, Life Technologies) with ABI 7500 Real-Time PCR system (Applied Biosystems) using primers listed in Table S2.

### RNA-Seq Library Preparation and Gene Expression Level Analysis

Oocytes were collected from 3-week-old and 3-month-old WT and *Cxhc1<sup>fl/fl</sup>;Zp3-Cre* female mice. Zygotes were collected from WT and *Cxhc1<sup>fl/fl</sup>;Zp3-Cre* mice after superovulation and mating with WT males (60 oocytes or zygotes per sample). After picking the cells into 350 µL lysis buffer supplied in RNeasy micro kit (QIAGEN), 3 × 10<sup>7</sup> ERCC molecules

were added into the lysis buffer. Total RNA was extracted with the RNeasy micro kit (QIAGEN) following the manual. Libraries were prepared with NEBNext Ultra RNA Library Prep Kit for Illumina. The libraries were sequenced on an Illumina platform with 150-bp pair-end reads. We used a perlscript to filter out low-quality reads, and then the clean reads were mapped to mouse genome mm10 with TopHat (version 2.0.6). Gene expression levels were calculated and normalized to FPKM using cuffquant and cuffnorm. Absolute mRNA copy number is calculated by spiked-in ERCC. FPKM and mRNA copy number both represent the gene expression level.

### Expression Level Comparison between WT and CFP1-Deleted Zygotes

The genes that were at least detected in all samples with FPKM >0.1 were arranged according to their mean expression in WT GV oocyte samples. And then these genes were divided into ten or five equal-sized bins. The averaged mRNA copy number of each gene within replicates was calculated, and then the relative expressions for each gene were calculated as copy number in each replicate to the average number of WT\_GV oocytes. Afterward, the embryo samples were plotted with boxplot in R. In the same way, the relative expression ratio of zygote to GV oocyte for each filtered gene in the bins was plotted. We used edgeR in R (version 3.2.5) to search for genes differentially expressed between WT and CFP1-deleted oocytes and identified genes upregulated and downregulated in CFP1-deleted oocytes as FC[WT/CFP1-deleted]  $\leq 0.5$  or  $\geq 2$ , p value <0.05, FDR <0.05.

### Category of Genes during Oocyte-to-Zygote Development and GSEA Analysis

We first find out the differentially expressed genes (DEGs) between WT GV oocytes and zygotes using edgeR. Genes with FC[zygote/GV]  $\leq 0.5$ , p value <0.05, FDR <0.05 were recognized as GV-Zygote decreased genes, while those with FC[zygote/GV]  $\geq 2$ , p value <0.05, FDR <0.05 were GV-Zygote increased genes. GV-Zygote stable genes were those with log2(FC [WT/CFP1-deleted]) between -0.5 to 0.5. The table of converted mRNA abundance that contains both WT and *Cxhc1<sup>fl/fl</sup>;Zp3-Cre* GV oocyte and zygote samples were uploaded to the GSEA software, and the GV-Zygote decreased genes were uploaded as gene set database. We set phenotype as permutation type, so the significant FDR cutoff could be 0.25 according to the GSEA user guide. GSEA result shows the enrichment of one specific set of genes in WT or *Cxhc1<sup>fl/fl</sup>;Zp3-Cre* samples.

### Statistical Analysis

The experiments were randomized and were performed with blinding to the conditions of the experiments. No statistical method was used to predetermine sample size. Informed content was obtained from all subjects. Results are given as means  $\pm$  SEM. Each experiment included at least three independent samples and was repeated at least three times. Results for two experimental groups were compared by two-tailed unpaired Student's t tests. Statistically significant values were \*p < 0.05, \*p < 0.01, and \*p < 0.001.

### ACCESSION NUMBERS

The accession number for the data sets reported in this paper is GEO: GSE85019.

### SUPPLEMENTAL INFORMATION

Supplemental Information includes Supplemental Experimental Procedures, five figures, and three tables and can be found with this article online at <http://dx.doi.org/10.1016/j.celrep.2017.07.011>.

### AUTHOR CONTRIBUTIONS

H.-Y.F., C.Y., and F.T. conceived the project and designed the experiments. C.Y. performed and analyzed the bulk of the experiments. X.F. and F.T. performed and analyzed the RNA-seq. H.-H.W. and L.S. assisted the analyses of sequencing data. Q.-Q.S. did the microinjection and immunostaining of

histone variants. B.-T.L., X.-X.D., and J.L. helped to perform the experiments. L.W. provided the *Cxhc1*-floxed mice. C.Y. and H.-Y.F. wrote the manuscript, while K.L. and F.T. revised it.

### ACKNOWLEDGMENTS

This study is funded by the National Key Research and Development Program of China (2016YFC1000600 and 2017YFSF1001500) and the National Natural Science Foundation of China (31528016, 91519313, 31371449, and 31671558).

Received: March 21, 2017

Revised: May 22, 2017

Accepted: July 6, 2017

Published: August 1, 2017

### REFERENCES

- Akiyama, T., Suzuki, O., Matsuda, J., and Aoki, F. (2011). Dynamic replacement of histone H3 variants reprograms epigenetic marks in early mouse embryos. *PLoS Genet.* 7, e1002279.
- Ancelin, K., Syx, L., Borensztein, M., Ranisavljevic, N., Vassilev, I., Briseño-Roa, L., Liu, T., Metzger, E., Servant, N., Barillot, E., et al. (2016). Maternal LSD1/KDM1A is an essential regulator of chromatin and transcription landscapes during zygotic genome activation. *eLife*, Published online Feb 2, 2016. <http://dx.doi.org/10.7554/eLife.08851>.
- Andreu-Vieyra, C.V., Chen, R., Agno, J.E., Glaser, S., Anastassiadis, K., Stewart, A.F., and Matzuk, M.M. (2010). MLL2 is required in oocytes for bulk histone 3 lysine 4 trimethylation and transcriptional silencing. *PLoS Biol.* Published online August 17, 2010. <http://dx.doi.org/10.1371/journal.pbio.1000453>.
- Aoshima, K., Inoue, E., Sawa, H., and Okada, Y. (2015). Paternal H3K4 methylation is required for minor zygotic gene activation and early mouse embryonic development. *EMBO Rep.* 16, 803–812.
- Barrera, L.O., Li, Z., Smith, A.D., Arden, K.C., Cavenee, W.K., Zhang, M.Q., Green, R.D., and Ren, B. (2008). Genome-wide mapping and analysis of active promoters in mouse embryonic stem cells and adult organs. *Genome Res.* 18, 46–59.
- Butler, J.S., Lee, J.H., and Skalnik, D.G. (2008). CFP1 interacts with DNMT1 independently of association with the Setd1 Histone H3K4 methyltransferase complexes. *DNA Cell Biol.* 27, 533–543.
- Cao, W., Guo, J., Wen, X., Miao, L., Lin, F., Xu, G., Ma, R., Yin, S., Hui, Z., Chen, T., et al. (2016). CXXC finger protein 1 is critical for T-cell intrathymic development through regulating H3K4 trimethylation. *Nat. Commun.* 7, 11687.
- Carlone, D.L., and Skalnik, D.G. (2001). CpG binding protein is crucial for early embryonic development. *Mol. Cell Biol.* 21, 7601–7606.
- Ciccone, D.N., Su, H., Hevi, S., Gay, F., Lei, H., Bajko, J., Xu, G., Li, E., and Chen, T. (2009). KDM1B is a histone H3K4 demethylase required to establish maternal genomic imprints. *Nature* 461, 415–418.
- Clouaire, T., Webb, S., Skene, P., Illingworth, R., Kerr, A., Andrews, R., Lee, J.H., Skalnik, D., and Bird, A. (2012). Cfp1 integrates both CpG content and gene activity for accurate H3K4me3 deposition in embryonic stem cells. *Genes Dev.* 26, 1714–1728.
- Clouaire, T., Webb, S., and Bird, A. (2014). Cfp1 is required for gene expression-dependent H3K4 trimethylation and H3K9 acetylation in embryonic stem cells. *Genome Biol.* 15, 451.
- Dahl, J.A., Jung, I., Aanes, H., Greggains, G.D., Manaf, A., Lerdrup, M., Li, G., Kuan, S., Li, B., Lee, A.Y., et al. (2016). Broad histone H3K4me3 domains in mouse oocytes modulate maternal-to-zygotic transition. *Nature* 537, 548–552.
- Gu, T.P., Guo, F., Yang, H., Wu, H.P., Xu, G.F., Liu, W., Xie, Z.G., Shi, L., He, X., Jin, S.G., et al. (2011). The role of Tet3 DNA dioxygenase in epigenetic reprogramming by oocytes. *Nature* 477, 606–610.
- Hajkova, P., Jeffries, S.J., Lee, C., Miller, N., Jackson, S.P., and Surani, M.A. (2010). Genome-wide reprogramming in the mouse germ line entails the base excision repair pathway. *Science* 329, 78–82.

- Kim, B., Kan, R., Anguish, L., Nelson, L.M., and Coonrod, S.A. (2010). Potential role for MATER in cytoplasmic lattice formation in murine oocytes. *PLoS ONE* 5, e12587.
- Kim, B., Zhang, X., Kan, R., Cohen, R., Mukai, C., Travis, A.J., and Coonrod, S.A. (2014). The role of MATER in endoplasmic reticulum distribution and calcium homeostasis in mouse oocytes. *Dev. Biol.* 386, 331–339.
- Kim, J., Singh, A.K., Takata, Y., Lin, K., Shen, J., Lu, Y., Kerényi, M.A., Orkin, S.H., and Chen, T. (2015). LSD1 is essential for oocyte meiotic progression by regulating CDC25B expression in mice. *Nat. Commun.* 6, 10116.
- LaVoie, H.A. (2005). Epigenetic control of ovarian function: The emerging role of histone modifications. *Mol. Cell. Endocrinol.* 243, 12–18.
- Lee, J.H., and Skalnik, D.G. (2005). CpG-binding protein (CXXC finger protein 1) is a component of the mammalian Set1 histone H3-Lys4 methyltransferase complex, the analogue of the yeast Set1/COMPASS complex. *J. Biol. Chem.* 280, 41725–41731.
- Lepikhov, K., and Walter, J. (2004). Differential dynamics of histone H3 methylation at positions K4 and K9 in the mouse zygote. *BMC Dev. Biol.* 4, 12.
- Lewandoski, M., Wassarman, K.M., and Martin, G.R. (1997). Zp3-cre, a transgenic mouse line for the activation or inactivation of loxP-flanked target genes specifically in the female germ line. *Curr. Biol.* 7, 148–151.
- Li, L., Baibakov, B., and Dean, J. (2008). A subcortical maternal complex essential for preimplantation mouse embryogenesis. *Dev. Cell* 15, 416–425.
- Li, L., Lu, X., and Dean, J. (2013). The maternal to zygotic transition in mammals. *Mol. Aspects Med.* 34, 919–938.
- Lin, C.J., Koh, F.M., Wong, P., Conti, M., and Ramalho-Santos, M. (2014). Hira-mediated H3.3 incorporation is required for DNA replication and ribosomal RNA transcription in the mouse zygote. *Dev. Cell* 30, 268–279.
- Liu, X., Wang, C., Liu, W., Li, J., Li, C., Kou, X., Chen, J., Zhao, Y., Gao, H., Wang, H., et al. (2016a). Distinct features of H3K4me3 and H3K27me3 chromatin domains in pre-implantation embryos. *Nature* 537, 558–562.
- Liu, Y., Lu, X., Shi, J., Yu, X., Zhang, X., Zhu, K., Yi, Z., Duan, E., and Li, L. (2016b). BTG4 is a key regulator for maternal mRNA clearance during mouse early embryogenesis. *J. Mol. Cell Biol.* 8, 366–368.
- Long, H.K., Blackledge, N.P., and Klose, R.J. (2013). ZF-CxxC domain-containing proteins, CpG islands and the chromatin connection. *Biochem. Soc. Trans.* 41, 727–740.
- Lucifero, D., Mertineit, C., Clarke, H.J., Bestor, T.H., and Trasler, J.M. (2002). Methylation dynamics of imprinted genes in mouse germ cells. *Genomics* 79, 530–538.
- Nashun, B., Hill, P.W., Smallwood, S.A., Dharmalingam, G., Amouroux, R., Clark, S.J., Sharma, V., Ndjetehe, E., Pelczar, P., Festenstein, R.J., et al. (2015). Continuous histone replacement by Hira is essential for normal transcriptional regulation and de novo DNA methylation during mouse oogenesis. *Mol. Cell* 60, 611–625.
- Schaefer, C.B., Ooi, S.K., Bestor, T.H., and Bourc'his, D. (2007). Epigenetic decisions in mammalian germ cells. *Science* 316, 398–399.
- Tashiro, F., Kanai-Azuma, M., Miyazaki, S., Kato, M., Tanaka, T., Toyoda, S., Yamato, E., Kawakami, H., Miyazaki, T., and Miyazaki, J. (2010). Maternal-effect gene *Ces5/Ooep/Moep19/Floped* is essential for oocyte cytoplasmic lattice formation and embryonic development at the maternal-zygotic stage transition. *Genes Cells* 15, 813–828.
- Tate, C.M., Lee, J.H., and Skalnik, D.G. (2010). CXXC finger protein 1 restricts the Setd1A histone H3K4 methyltransferase complex to euchromatin. *FEBS J.* 277, 210–223.
- Thomson, J.P., Skene, P.J., Selfridge, J., Clouaire, T., Guy, J., Webb, S., Kerr, A.R., Deaton, A., Andrews, R., James, K.D., et al. (2010). CpG islands influence chromatin structure via the CpG-binding protein Cfp1. *Nature* 464, 1082–1086.
- Wasson, J.A., Simon, A.K., Myrick, D.A., Wolf, G., Driscoll, S., Pfaff, S.L., Macfarlan, T.S., and Katz, D.J. (2016). Maternally provided LSD1/KDM1A enables the maternal-to-zygotic transition and prevents defects that manifest postnatally. *eLife*, Published online January 27, 2016. <http://dx.doi.org/10.7554/eLife.08848>.
- Wu, D., and Dean, J. (2016). BTG4, a maternal mRNA cleaner. *J. Mol. Cell Biol.* 8, 369–370.
- Yu, C., Ji, S.Y., Sha, Q.Q., Sun, Q.Y., and Fan, H.Y. (2015). CRL4-DCAF1 ubiquitin E3 ligase directs protein phosphatase 2A degradation to control oocyte meiotic maturation. *Nat. Commun.* 6, 8017.
- Yu, C., Ji, S.Y., Sha, Q.Q., Dang, Y., Zhou, J.J., Zhang, Y.L., Liu, Y., Wang, Z.W., Hu, B., Sun, Q.Y., et al. (2016). BTG4 is a meiotic cell cycle-coupled maternal-zygotic-transition licensing factor in oocytes. *Nat. Struct. Mol. Biol.* 23, 387–394.
- Zhang, B., Zheng, H., Huang, B., Li, W., Xiang, Y., Peng, X., Ming, J., Wu, X., Zhang, Y., Xu, Q., et al. (2016). Allelic reprogramming of the histone modification H3K4me3 in early mammalian development. *Nature* 537, 553–557.
- Zhao, X.D., Han, X., Chew, J.L., Liu, J., Chiu, K.P., Choo, A., Orlov, Y.L., Sung, W.K., Shahab, A., Kuznetsov, V.A., et al. (2007). Whole-genome mapping of histone H3 Lys4 and 27 trimethylations reveals distinct genomic compartments in human embryonic stem cells. *Cell Stem Cell* 1, 286–298.